modulation function. Together with the decreasing amplitude of the atoms this points towards an ordinary crystal structure, which is reached at the transformation point.

This phase transformation is a further example of incommensurate–commensurate transformations. The strong variation of the reflection intensities with pressure allowed an accurate examination of the changing structural properties under high pressure. For further investigations it would be interesting to examine the influence of silver on the phase transformation.

This work was supported by the Bundesminister für Forschung und Technologie, grant No. 05 464 IBB9.

References

CHERIN, P. & UNGER, P. (1967). *Acta Cryst.* **23**, 670–671.
DAM, B., JANNER, A. & DONNAY, J. D. H. (1985). *Phys. Rev. Lett.* **55**, 2301–2304.
FINGER, L. W. & KING, H. (1978). *Am. Mineral.* **63**, 337.
HAMILTON, W. C. (1965). *Acta Cryst.* **18**, 502–510.
JANNER, A. & DAM, B. (1989). *Acta Cryst.* A**45**, 115–123.
KÖPKE, J. & SCHULZ, H. (1986). *Phys. Chem. Miner.* **13**, 165–173.
KUPCIK, V., WENDSCHUH-JOSTIES, M., WOLF, A. & WULF, R. (1986). *Nucl. Instrum. Methods*, A**246**, 624–626.
MERRILL, L. & BASSETT, W. A. (1974). *Rev. Sci. Instrum.* **45**, 290–294.
PIERMARINI, G. J., BLOCK, S. & BARNETT, J. D. (1973). *J. Appl. Phys.* **44**, 5377–5382.
PIERMARINI, G. J., BLOCK, S., BARNETT, J. D. & FORMAN, R. D. (1975). *J. Appl. Phys.* **46**, 2774–2780.
REITHMAYER, K., STEURER, W., SCHULZ, H. & DE BOER, J. L. (1990). *Acta Cryst.* A**46**, C-393–C-394.
SCHUTTE, W. J. & DE BOER, J. L. (1988). *Acta Cryst.* B**44**, 486–494.
TRIEST, A. VAN, FOLKERTS, W. & HAAS, C. (1990). *J. Phys. Condens. Matter*, **2**, 8733–8740.
TUNELL, G. & PAULING, L. (1952). *Acta Cryst.* **5**, 375–381.
VAN TENDELOO, G., AMELINCKX, S. & GREGORIADES, P. (1984). *J. Solid State Chem.* **53**, 281–289.
VAN TENDELOO, G., GREGORIADES, P. & AMELINCKX, S. (1983). *J. Solid State Chem.* **50**, 321–334, 335–361.
YAMAMOTO, A. (1982). *REMOS*82.0. *Computer Program for the Refinement of Modulated Structures.* National Institute for Research in Inorganic Materials, Sakura-mura, Niihari-gun, Ibaraki 305, Japan.
ZUCKER, U., PERENTHALER, E., KUHS, W. F., BACHMANN, R. & SCHULZ, H. (1983). *J. Appl. Cryst.* **16**, 358.

Acta Cryst. (1993). B**49**, 11–18

Thermal Vibrations of Atoms and Phase Transition in $RbHSeO_4$ and NH_4HSeO_4 Single Crystals

BY I. P. MAKAROVA

Institute of Crystallography, Academy of Sciences, Leninsky pr. 59, 117333 *Moscow, Russia*

(*Received* 16 *January* 1992; *accepted* 5 *June* 1992)

Abstract

Using neutron diffraction data on single crystals of $RbHSeO_4$ in the paraelectric phase at 383 K and in the ferroelectric phase at 293 K, and NH_4HSeO_4 crystals in the paraelectric phase at 293 and 400 K, the thermal vibration parameters of the atoms in these crystals as well as the structural changes in $RbHSeO_4$ during the ferroelectric phase transition have been studied. The phase transitions in these crystals are due to ordering of the H-atom arrangement for one of the hydrogen bonds.

Introduction

Similar sequences of phase transitions have been found in $RbHSeO_4$ and NH_4HSeO_4 crystals (Poprawski, Mroz, Czapla & Sobczyk, 1979; Czapla, Lis & Sobczyk, 1979; Rozanov, Moskvitch, Sukhovsky & Aleksandrova, 1983; Czapla, 1982; Suzuki, Osaka & Makita, 1979; Moskvitch, Sukhovsky & Rozanov, 1984; Aleksandrova, Blat, Zinenko, Moskvitch & Sukhovsky, 1987). Replacement of the Rb atom by the $[NH_4]$ group lowers the ferroelectric phase transition temperature by 120 K (from 370 to 250 K) (Poprawski, Mroz, Czapla & Sobczyk, 1979; Czapla, Lis & Sobczyk, 1979). X-ray structural studies of the paraelectric and ferroelectric phases provide reliable information on the heavy atoms (Waśkowska, Olejnik, Łukaszewicz & Czapla, 1980; Waśkowska, Olejnik, Łukaszewicz & Głowiak, 1978; Aleksandrov, Kruglik, Misul & Simonov, 1980; Kruglik, Misul & Aleksandrov, 1980) and show that the corresponding phases of these crystals are isostructural. The accuracy of the X-ray diffraction data was however insufficient to locate the H atoms and to study the changes in the hydrogen bonds during the phase transitions. NMR data on ^{77}Se suggested that the ferroelectric phase transition in these crystals is due

0108-7681/93/010011-08$06.00

Table 1. *Crystal data*

Reliability factors: $wR^2 = \sum_{hkl} w(F_{obs} - F_{calc})^2 / \sum_{hkl} wF_{obs}^2$, $R = \sum_{hkl} |F_{obs} - F_{calc}| / \sum_{hkl} F_{obs}$, weights $w = 1/\sigma^2(F_{obs})$.

	RbHSeO$_4$		NH$_4$HSeO$_4$	
	383 K	293 K	400 K	293 K
Space group	*B*2	*B*1	*B*2	*B*2
a (Å)	19.962 (9)	19.852 (8)	19.863 (13)	19.754 (8)
b (Å)	4.634 (2)	4.622 (1)	4.620 (3)	4.607 (1)
c (Å)	7.611 (3)	7.575 (3)	7.593 (7)	7.550 (2)
α (°)	90.0	90.64 (3)	90.0	90.0
β (°)	90.0	90.04 (3)	90.0	90.0
γ (°)	102.76 (3)	102.75 (3)	102.59 (5)	102.59 (3)
V (Å^3)	686.7 (4)	677.9 (4)	680.1 (9)	670.5 (4)
Z	6	6	6	6
D_x (g cm^{-3})	3.328	3.371	2.373	2.407
Reciprocal space	$+h, \pm k, +l$	$+h, \pm k, \pm l$	$+h, \pm k, \pm l$	$+h, \pm k, \pm l$
Max. $\sin\theta/\lambda$ (Å^{-1})	0.79	0.79	0.79	0.79
Scan mode	$\theta/2\theta$	$\theta/2\theta$	$\theta/2\theta$	$\theta/2\theta$
Reflections measured	1088	2339	897	1285
Unique reflections ($I > 3\sigma_I$)	1069	2317	532	744
Agreement factor on I, R_{int}	–	–	0.060	0.056
μ (cm^{-1})	0.076	0.077	0.090	0.092
g^* ($\times 10^6$)	0.281 (5)	0.609 (7)	1.55 (2)	1.38 (2)
wR	0.053	0.053	0.055	0.051
R	0.039	0.044	0.054	0.047

* Isotropic extinction corrections, Becker & Coppens formalism, type I, Lorentzian distribution.

to ordering of H-atom positions on the hydrogen bonds (Rozanov, Moskvitch & Sukhovsky, 1983; Czapla, Lis, Sobczyk, Waśkowska, Mroz & Poprawski, 1980). Brach, Jones & Roziere (1983) carried out a neutron diffraction study on RbHSeO$_4$ crystals at 387 K in the paraelectric phase and confirmed that the H atoms are disordered.

The aim of this work is to investigate the structural reconstruction during the ferroelectric phase transition and the changes in hydrogen bonding using neutron diffraction data on single crystals of RbHSeO$_4$ and NH$_4$HSeO$_4$ at various temperatures.

Refinement of structural models

We have carried out a neutron diffraction study of RbHSeO$_4$ crystals in the paraelectric phase at 383 K and in the ferroelectric phase at 293 K, and NH$_4$HSeO$_4$ crystals in the paraelectric phase at 293 and 400 K. The main crystal data are listed in Table 1.* To facilitate comparison of the ferroelectric and paraelectric phases, we used a unit cell in the ferroelectric phase in a non-standard setting *B*1. The lattice parameters for the standard setting *P*1 are: $a = 10.622$ (4), $b = 4.622$ (1), $c = 7.575$ (3) Å, $\alpha = 89.35$ (3), $\beta = 110.84$ (3), $\gamma = 102.13$ (3)°. The setting *P*1 is transformed to *B*1 according to the equations: $\mathbf{a}_B = -2\mathbf{a}_P - \mathbf{c}_P$, $\mathbf{b}_B = -\mathbf{b}_P$, $\mathbf{c}_B = \mathbf{c}_P$.

The experimental neutron diffraction data were obtained from spherical specimens of RbHSeO$_4$ and NH$_4$HSeO$_4$ crystals 7 and 6 mm in diameter, respectively, on a Syntex $P\bar{1}$ automatic diffractometer in the VVR-C reactor ($\lambda = 1.1674$ Å) (Makarova, Rider, Sarin, Aleksandrova & Simonov, 1989; Makarova, Muradyan, Rider, Sarin, Aleksandrova & Simonov, 1990). Intensities of diffraction reflections with $I > 3\sigma_I$ were converted to moduli of structure amplitudes taking into account the Lorentz factor and absorption. Refinement of the structural models as well as all other calculations were carried out using the *PROMETHEUS* program system (Zucker, Perenthaler, Kuhs, Bachmann & Schulz, 1983). Extinction was allowed for in the isotropic approximation according to the Becker & Coppens (1974) formalism.

For all the above phases the structural models were initially refined without taking account of the H atoms. Fig. 1 shows the projection of the RbHSeO$_4$ structure on the xy plane in the paraelectric phase. The structures are based on [SeO$_4$] tetrahedra, linked by hydrogen bonds so as to form chains extending along the y axis. These chains are interlinked by Rb atoms (in NH$_4$HSeO$_4$ by [NH$_4$] groups). As for the paraelectric phase, the asymmetric unit contains two symmetrically nonequivalent groups: [Se(1)O$_4$], lying on the twofold axis, and [Se(2)O$_4$] in the general position. The former are joined by hydrogen bonds of the α type, the latter by β-type bonds. In the

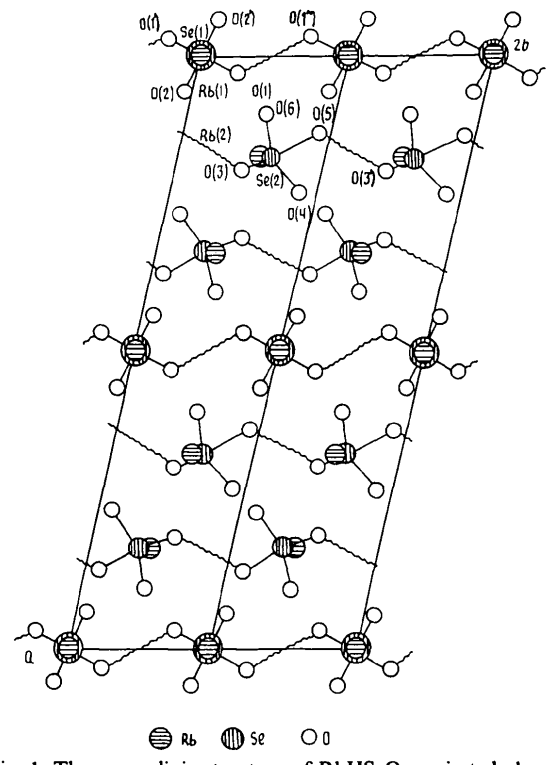

Fig. 1. The monoclinic structure of RbHSeO$_4$ projected along the twofold axis (z). The hydrogen bonds are shown as wavy lines.

* Lists of structure factors and anisotropic thermal parameters have been deposited with the British Library Document Supply Centre as Supplementary Publication No. SUP 55445 (92 pp.). Copies may be obtained through The Technical Editor, International Union of Crystallography, 5 Abbey Square, Chester CH1 2HU, England. [CIF reference: SH0005]

ferroelectric phase there are three symmetrically nonequivalent [SeO_4] groups, because disappearance of the twofold axis leads to nonequivalence of two [Se(2)O_4] tetrahedra, denoted below as [Se(2)O_4] and [Se(22)O_4]. Here and below, indices of the type *'l'* and *'ll'* indicate the positions of atoms which were symmetrically equivalent with respect to the twofold axis in the paraelectric phase.

After refinement of the structural models without taking the H atoms into account, difference nuclear density maps were constructed. Fig. 2 shows the nuclear density map in planes of (*a*) α-type and (*b*) β-type hydrogen bonds for $RbHSeO_4$ in the paraelectric phase at 383 K. For NH_4HSeO_4 the nuclear density maps are just the same and are not given here. The H distributions of the α and β bonds differ significantly. The peak corresponding to the H(2) atom is spherically symmetrical and compact. The hydrogen β bond O(5)—H(2)···O(3′) has a typical asymmetrical geometry. The O(5) atom emerges uniquely as the donor. The peak corresponding to the H(1) atom is diffuse and extended along the α bond O(1)—O(1″). The extremum value of nuclear density is found on the twofold axis, the appropriate point of the axis being the middle of the α bond. The value of this extremum is about 1.5 times less than the corresponding value for the H(2) atom. This extremum can be interpreted as a superposition of densities corresponding to two H(1) sites populated with a probability of $\frac{1}{2}$ [these sites are marked $H(1)_2$ and $H(1')_2$ in Fig. 2]. This two-site model provides an asymmetrical geometry of the hydrogen bonds O(1)—$H(1)_2$···O(1″), O(1)···$H(1')_2$—O(1″) and agrees with the data of the structural investigation of $RbHSeO_4$ carried out by Brach, Jones & Roziere (1983).

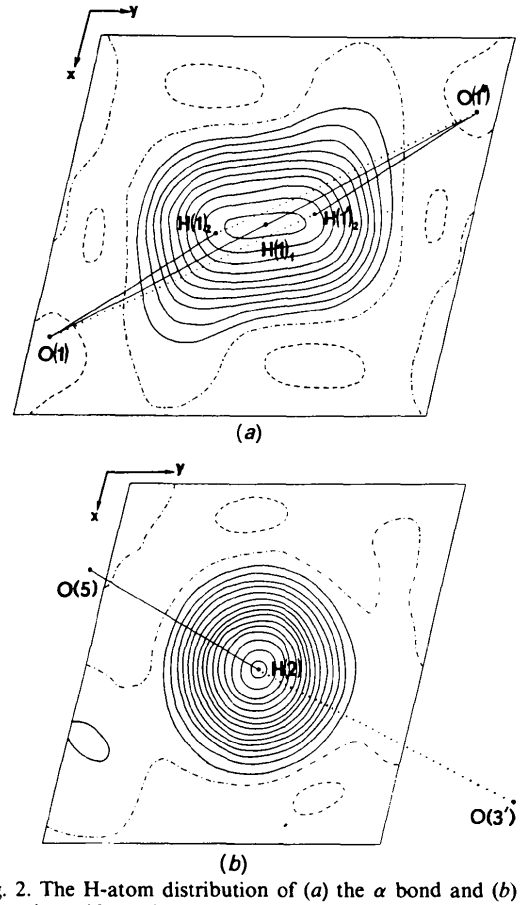

Fig. 2. The H-atom distribution of (*a*) the α bond and (*b*) the β bond at 383 K in $RbHSeO_4$ in the *xy* plane. Contours at 0.5 fm $Å^{-3}$. Solid lines connect points with the same negative density (hydrogen has negative neutron scattering length), dashed lines – with the same positive density, dotted-and-dashed lines – with zero density.

Another possible interpretation of the H distribution is the arrangement of the H(1) atom on the twofold axis with anomalously large thermal motion amplitudes and a possible anharmonicity. From the existing approaches to the calculation of anharmonicity of thermal vibrations we choose the the Gram–Charlier expansion (Muradyan, Sirota, Makarova & Simonov, 1985). The temperature factor T(H) with allowance for anharmonicity is written in terms of the Fourier transform of the probability density function $p(X)$, with allowance in the expansion for not only the harmonic terms, but also for the anharmonic components of third and higher orders. Adding the anharmonic terms increases the number of refineable parameters for each basis atom of the structure. The anharmonic parameters included in refinement require special attention, since they are correlated both mutually and with the positional and harmonic thermal parameters of the atom. In the refinement we introduced tensors of the temperature factor up to fourth order; this, even with the limitation imposed by the point symmetry of the position, gives 17 refined parameters for the H(1) atom. The experience of precise structural investigations shows that the number of significant parameters is considerably lower. To identify the significant parameters of thermal vibration under the conditions of a marked correlation and limited amount of experimental data we used the following procedure. In the first stages of the refinement we varied all the non-zero components of the thermal tensors according to the conditions of symmetry. Then the components, which in absolute value did not exceed their standard deviations and did not reduce the R factor, were set equal to zero and were not included in the subsequent stages of refinement. This procedure enabled us to reveal and to take into account only the significant components of the tensors: for $RbHSeO_4$ at 383 K $D^{2222} = -0.36\,(4) \times 10^{-4}$, $D^{1222} = 0.019\,(6) \times 10^{-4}$; for NH_4HSeO_4 at 293 K $D^{2222} = -0.27\,(5) \times 10^{-4}$, $D^{1222} = 0.020\,(8) \times 10^{-4}$.

From the results of the refinement of the anharmonic model we obtained the effective one-particle potential for the H(1) atom (Fig. 3). The anharmonic potential distribution exhibits two minima which correspond to the $H(1)_2$ and $H(1')_2$ sites in the two-site harmonic model of the structure. In the paraelectric phase of NH_4HSeO_4 at 400 K we did not obtain significant anharmonic parameters, which is probably associated with sufficient additional heat energy of the H(1) atom to exceed the potential barrier.

Refinement of the two structural models (the two-site harmonic model and the anharmonic model) led to equal R factors for each case, although the anharmonic model contains less parameters. Note that the choice of any of the models for H(1) disorder does not influence the results of refinement of the parameters of all the remaining atoms. Thus in this case we came across a situation which is fairly often encountered, in which using diffraction methods it is impossible to determine a preference for one of the models purely from the value of the R factor. This situation is related to the fact that for a small displacement Δx of an atom the value $\cos(2\pi h\Delta x)$ which influences structural amplitudes can always be compensated for, to a high degree of accuracy, by the thermal factor $\exp(-\Delta Bh)$ with $\Delta B = \frac{1}{2}(2\pi\Delta x)^2$. Additional information is required for a final choice of structural model.

Detailed analysis of the ferroelectric phase transition has been carried out for $RbHSeO_4$ crystals. At 293 K the $RbHSeO_4$ crystal is in the ferroelectric phase and one would expect twinning of the specimen. Careful analysis of the diffraction pattern and reflection intensity differences led unambiguously to triclinic symmetry of the ferroelectric phase and at the first stage of the refinement we assumed the sample to be a single domain. Non-H atoms in the ferroelectric phase were refined based on this assumption. Three H atoms were localized on difference density maps. Two hydrogen bonds of the β type [the H(2) and H(22) atoms] which became crystallographically independent turned out to be similar in their geometry. Changes in the nuclear density of the H(1) atom on the α bond accompanying the phase transition are evident if we compare Figs. 2 and 4. A much more compact peak corresponds to the H(1) atom on the difference map at 293 K as compared to 383 K; it is equal in height to the peaks corresponding to the H(2) and H(22) atoms. The site of the extremum has virtually shifted to the $H(1')_2$ site of the paraelectric phase. Analysis of the difference density map shown in Fig. 4 reveals asphericity of the peak corresponding to the H(1) atom. Refinement of the model with H-atom disorder did not reduce the R factor. Naturally, we can suppose that the asphericity is due to the presence of second orientation domains in the sample which we first considered to be a single domain. In the course of refinement of the structure, with allowance for twinning, we used a least-squares method for the analysis of twins (Sirota & Maksimov, 1984, Kondratyuk, Loshmanov, Muradyan, Maksimov, Sirota, Krivandina & Sobolev, 1988) and, for the specimen investigated, obtained the twin volume ratio $V_1:V_2 = 7.4:1.0$. The H-atom distribution obtained in the ferroelectric phase displays a change in the α bond: it becomes asymmetrical and equivalent in geometry to the β bond.

Refined structural parameters of $RbHSeO_4$ and NH_4HSeO_4 crystals (for the ferroelectric phase of $RbHSeO_4$ with allowance for twinning) are given in Table 2. The main interatomic distances and angles are listed in Table 3.

Discussion

Comparison of the structures of the paraelectric phases of $RbHSeO_4$ at 383 K and NH_4HSeO_4 at 293 and 400 K (Table 3) reveals a complete similarity of the geometry of the $[SeO_4]$ tetrahedra and the corre-

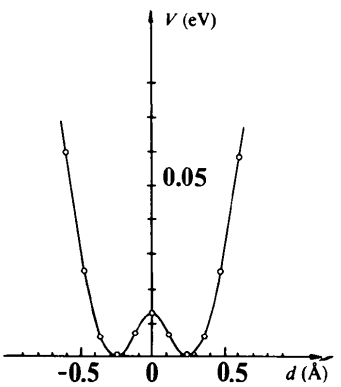

Fig. 3. One-particle potential for the H(1) atom in the O(1)—O(1'') bond direction in the NH_4HSeO_4 crystal at 293 K.

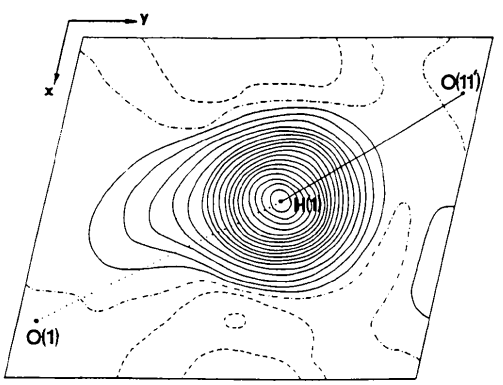

Fig. 4. The H-atom distribution of the α bond in $RbHSeO_4$ at 293 K in the xy plane. Notation as in Fig. 2.

Table 2. *Structural parameters for* $RbHSeO_4$ *and* NH_4HSeO_4

The positional parameters are given in fractional coordinates. B_{eq} denotes the equivalent isotropic thermal parameter calculated from the vibrational ellipsoid volume in Å^2. Estimated standard deviations are given, in parentheses, on the last quoted place. The position of the Se(2) atom is fixed in the ferroelectric phase of $RbHSeO_4$ at 293 K. Two columns are reserved for $RbHSeO_4$ at 293 K to accommodate atoms *A(I)* and *A(II)* which are equivalent in the *B*2 phase. Parameters of the H(1) atom are given for the two-site model [$H(1)_2$] and for the single-site model [$H(1)_1$].

		$RbHSeO_4$			NH_4HSeO_4	
		383 K	293 K		400 K	293 K
Rb(1)[N(1)]						
	x	0	0.9998 (1)		0	0
	y	0	0.0027 (5)		0	0
	z	0.4876 (6)	0.4881 (3)		0.4800 (10)	0.4810 (9)
	B_{eq}	3.16 (5)	2.33 (2)		4.35 (20)	2.71 (7)
Rb(2)[N(2)]						
	x	0.16552 (9)	0.16535 (9)	0.83461 (9)	0.1652 (3)	0.1650 (1)
	y	0.5827 (5)	0.5788 (5)	0.4195 (5)	0.5807 (10)	0.5728 (8)
	z	0.0862 (5)	0.0852 (3)	0.0879 (3)	0.0899 (9)	0.0880 (8)
	B_{eq}	3.04 (3)	2.32 (3)	2.33 (2)	4.27 (9)	2.69 (5)
Se(1)	*x*	0	0.00129 (7)		0	0
	y	0	0.0101 (3)		0	0
	z	0	0.0000 (2)		0	0
	B_{eq}	2.04 (3)	1.53 (2)		2.40 (10)	1.46 (6)
Se(2)	*x*	0.16745 (8)	0.16745	0.83259 (7)	0.1675 (3)	0.1676 (1)
	y	0.6983 (3)	0.6983	0.2995 (3)	0.6962 (9)	0.6991 (7)
	z	0.5768 (5)	0.5768	0.5776 (2)	0.5777 (8)	0.5784 (7)
	B_{eq}	2.17 (2)	1.70 (2)	1.73 (2)	2.92 (8)	1.75 (4)
O(1)	*x*	0.0294 (1)	0.0302 (1)	0.9703 (1)	0.0289 (5)	0.0301 (3)
	y	0.2846 (6)	0.2884 (5)	0.7163 (5)	0.287 (1)	0.284 (1)
	z	0.8654 (5)	0.8695 (3)	0.8603 (3)	0.865 (1)	0.8634 (9)
	B_{eq}	2.99 (4)	2.22 (3)	2.25 (3)	4.1 (2)	2.36 (7)
O(2)	*x*	0.0632 (1)	0.0628 (1)	0.9359 (1)	0.0637 (5)	0.0635 (3)
	y	0.9450 (7)	0.9378 (7)	0.0499 (7)	0.945 (2)	0.941 (1)
	z	0.1163 (5)	0.1190 (3)	0.1160 (3)	0.116 (1)	0.1174 (9)
	B_{eq}	3.39 (5)	2.58 (4)	2.68 (4)	4.4 (2)	2.74 (8)
O(3)	*x*	0.1938 (1)	0.1942 (1)	0.8055 (1)	0.1935 (5)	0.1939 (3)
	y	0.4706 (6)	0.4711 (5)	0.5281 (5)	0.468 (1)	0.468 (1)
	z	0.7100 (5)	0.7096 (4)	0.7113 (4)	0.710 (1)	0.7130 (9)
	B_{eq}	3.31 (5)	2.50 (3)	2.52 (3)	4.2 (2)	2.49 (8)
O(4)	*x*	0.2299 (2)	0.2303 (2)	0.7700 (1)	0.2295 (5)	0.2312 (3)
	y	0.9000 (7)	0.9011 (7)	0.0946 (7)	0.903 (2)	0.905 (1)
	z	0.4705 (6)	0.4704 (4)	0.4690 (4)	0.471 (1)	0.474 (1)
	B_{eq}	4.29 (7)	3.26 (5)	3.27 (5)	5.9 (2)	3.82 (10)
O(5)	*x*	0.1324 (2)	0.1318 (1)	0.8680 (1)	0.1323 (5)	0.1314 (3)
	y	0.9194 (6)	0.9202 (5)	0.0797 (5)	0.917 (1)	0.918 (1)
	z	0.7138 (6)	0.7149 (4)	0.7146 (4)	0.715 (1)	0.716 (1)
	B_{eq}	3.48 (5)	2.64 (4)	2.64 (4)	4.2 (2)	2.79 (9)
O(6)	*x*	0.1046 (2)	0.1045 (1)	0.8960 (1)	0.1060 (5)	0.1047 (3)
	y	0.5350 (8)	0.5314 (7)	0.4621 (7)	0.530 (2)	0.533 (1)
	z	0.4544 (6)	0.4522 (4)	0.4560 (4)	0.454 (1)	0.453 (1)
	B_{eq}	3.67 (6)	3.00 (4)	2.91 (4)	5.3 (2)	3.36 (10)
$H(1)_2$	*x*	0.0025 (9)	0.9964 (2)		0.001 (6)	0.003 (2)
	y	0.4466 (17)	0.5482 (9)		0.451 (10)	0.451 (3)
	z	0.8737 (14)	0.8718 (6)		0.873 (2)	0.871 (3)
	B_{eq}	3.5 (2)	2.73 (6)		7 (1)	2.9 (3)
$H(1)_1$	*x*	0			0	0
	y	0.05			0.5	0.5
	z	0.8737 (14)			0.873 (2)	0.871 (3)
	B_{eq}	5.0 (2)			8 (1)	4.1 (3)
H(2)	*x*	0.1581 (3)	0.1577 (2)	0.8417 (3)	0.1570 (7)	0.1564 (5)
	y	0.1328 (10)	0.1364 (10)	0.8637 (10)	0.130 (2)	0.134 (2)
	z	0.7078 (9)	0.7083 (7)	0.7083 (7)	0.710 (2)	0.709 (2)
	B_{eq}	3.84 (9)	3.23 (7)	3.27 (7)	4.9 (3)	3.1 (1)
H(3)	*x*				0.028 (2)	0.031 (1)
	y				0.928 (7)	0.906 (8)
	z				0.398 (4)	0.413 (4)
	B_{eq}				13 (1)	11 (1)

Table 2 (*cont.*)

		$RbHSeO_4$		NH_4HSeO_4	
		383 K	293 K	400 K	293 K
H(4)	*x*			0.028 (2)	0.032 (1)
	y			0.149 (5)	0.162 (5)
	z			0.534 (4)	0.520 (4)
	B_{eq}			14 (1)	11 (1)
H(5)	*x*			0.163 (2)	0.177 (3)
	y			0.543 (6)	0.511 (10)
	z			0.973 (2)	0.969 (3)
	B_{eq}			10 (2)	14 (2)
H(6)	*x*			0.139 (2)	0.143 (1)
	y			0.399 (8)	0.394 (9)
	z			0.116 (7)	0.134 (6)
	B_{eq}			15 (2)	15 (2)
H(7)	*x*			0.145 (2)	0.133 (1)
	y			0.649 (9)	0.695 (6)
	z			0.146 (7)	0.090 (6)
	B_{eq}			18 (2)	10 (2)
H(8)	*x*			0.200 (2)	0.208 (1)
	y			0.717 (9)	0.643 (9)
	z			0.126 (8)	0.138 (5)
	B_{eq}			18 (2)	12 (2)

Table 3. *Main interatomic distances* (Å) *and angles* (°) *in* $RbHSeO_4$ *and* NH_4HSeO_4 *crystals*

Parameters of the α bond are given for the two-site model. Two values in the column for the *P*1 phase of $RbHSeO_4$ (293 K) correspond to the distances which are equivalent in the *B*2 phase.

	$RbHSeO_4$			NH_4HSeO_4	
	383 K	293 K (one domain)		400 K	293 K
O(1)—O(1'')	2.530 (5)	2.524 (3)		2.48 (2)	2.53 (1)
O(1)—H(1)	1.02 (1)	1.030 (4)		1.04 (6)	1.03 (1)
O(1'')···H(1)	1.52 (1)	1.498 (4)		1.46 (5)	1.51 (1)
O(1)—H(1)—O(1'')	171 (1)	173.4 (4)		170 (3)	172 (2)
H(1)—H(1')	0.53 (2)	-		0.46 (6)	0.49 (2)
O(3')—O(5)	2.578 (4)	2.575 (3)	2.577 (3)	2.57 (1)	2.565 (6)
O(5)—H(2)	1.010 (5)	1.018 (5)	1.019 (5)	1.00 (1)	1.011 (9)
O(3')···H(2)	1.570 (5)	1.558 (5)	1.561 (5)	1.57 (1)	1.556 (9)
O(3')—H(2)—O(5)	175.3 (5)	175.9 (5)	175.2 (5)	177 (1)	176 (1)
Se(1)—O(1), O(1')	1.671 (3)	1.632 (3)	1.715 (2)	1.677 (7)	1.670 (5)
Se(1)—O(2), O(2')	1.607 (3)	1.611 (2)	1.613 (2)	1.608 (8)	1.607 (5)
Se(2)—O(3)	1.632 (3)	1.633 (3)	1.631 (3)	1.623 (8)	1.636 (5)
Se(2)—O(4)	1.603 (3)	1.608 (3)	1.606 (3)	1.603 (8)	1.606 (5)
Se(2)—O(5)	1.716 (3)	1.716 (3)	1.715 (3)	1.712 (8)	1.709 (5)
Se(2)—O(6)	1.611 (3)	1.614 (3)	1.612 (3)	1.599 (8)	1.616 (6)
O(1)—Se(1)—O(1')	104.4 (3)	104.6 (1)		104.6 (6)	103.8 (4)
O(1)—Se(1)—O(2), O(1')—Se(1)—O(2')	108.2 (2)	110.9 (2)	105.3 (2)	108.4 (4)	108.3 (3)
O(2)—Se(1)—O(2')	113.2 (3)	112.7 (2)		113.4 (6)	113.0 (4)
O(1)—Se(1)—O(2'), O(1')—Se(1)—O(2)	111.3 (1)	113.4 (1)	109.4 (1)	110.9 (4)	111.5 (2)
O(3)—Se(2)—O(4)	111.7 (2)	111.8 (2)	111.7 (2)	112.9 (6)	111.8 (4)
O(3)—Se(2)—O(5)	104.0 (2)	104.1 (2)	104.2 (2)	103.9 (4)	103.9 (3)
O(3)—Se(2)—O(6)	112.6 (2)	112.4 (2)	112.8 (2)	111.8 (4)	112.1 (3)
O(4)—Se(2)—O(5)	109.0 (2)	109.1 (2)	108.9 (2)	108.2 (4)	108.9 (3)
O(4)—Se(2)—O(6)	114.0 (2)	113.8 (2)	114.0 (2)	113.5 (5)	114.4 (4)
O(5)—Se(2)—O(6)	104.7 (2)	104.9 (2)	104.5 (2)	106.0 (6)	104.9 (3)

sponding hydrogen bonds. The differences in Se—O distances in the tetrahedra are due to structural features. In the $[Se(2)O_4]$ group the distances between the Se(2) and O(3), O(5) atoms engaged in β bonds exceed those between the Se(2) and O(4), O(6) atoms; Se(2)—O(3) and Se(2)—O(5) distances differ considerably and this difference is correlated with the func-

tions of the O atoms in the hydrogen β bonds: O(3) – acceptor, O(5) – donor. In the [Se(1)O_4] group on the twofold axis the distances between the Se(1) and O(1), O(1′) atoms involved in α bonds also exceed those between the Se(1) and O(2) atoms not involved in hydrogen bonds. These distances are equal to the averaged Se(2)—O(3) and Se(2)—O(5) distances. This result is to be expected, because the O(1) atoms perform the functions of donor or acceptor with a probability of $\frac{1}{2}$.

Analysis of the data presented in Table 3 shows that the principal changes taking place during the ferroelectric phase transition are due to the H(1)-atom ordering and appropriate transformations of the [Se(1)O_4] tetrahedra. In these tetrahedra the distances between the Se(1) atom and the O(2), O(22) atoms not involved in hydrogen bonds change insignificantly and remain the shortest ones. Ordering of the H(1) atom on the α bond causes the distances between the Se(1) and O atoms involved in hydrogen bonding to be no longer equivalent: the Se(1)—O(1) distance is reduced by 0.039 Å, while the Se(1)—O(11) distance is increased by 0.044 Å. Ordering of the H(1) atoms and transformation of the [Se(1)O_4] tetrahedra means that all [Se(1)O_4], [Se(2)O_4] and [Se(22)O_4] tetrahedra show similar distortions in the ferroelectric phase.

As mentioned above, it is impossible to choose one of the suggested models of the H(1) disorder on the α bond in the paraelectric phase proceeding only from the value of the R factor. Limited diffraction data do not provide a direct answer. However, analysis of the geometry of the α and β bonds and the thermal motion ellipsoids favour the model of anharmonic motion of the H(1) atom on the α bond. From Table 3 we see that the presence of hydrogen bonds with ordered H atoms leads to a regular difference between the lengths of Se—O bonds and this difference, which is correlated with the functions of the O atoms, is about 0.083 Å. From this viewpoint let us consider the two-site model for the H(1) atom on the α bond.

The two-site model with a static spatial disorder means that in each unit cell an equilibrium position of the H(1) atom corresponds to one of the two possible sites $H(1)_2$ or $H(1')_2$, hopping of H atoms from one of the sites to the other being rather rare. Therefore, the O(1) atoms play different roles (donor or acceptor) in different unit cells which is manifested in the Se—O bond length. We suppose that static spatial disorder of the H(1) atoms gives rise to local distortions of the [Se(1)O_4] tetrahedra in the paraelectric phase similar to the above-described distortions of the [Se(1)O_4] tetrahedra in the ferroelectric phase and comparable to the distortions of the [Se(2)O_4] tetrahedra which should be regarded as standard at the temperature of the investigation. The positional parameters of the O(1) atom in the averaged unit cell of the paraelectric phase would naturally correspond to a mean Se(1)—O(1) distance, while O(1)-atom disorder over the sites corresponding to the donor or acceptor functions would affect parameters of the thermal motion of this atom. Analysis of the thermal parameters obtained for the O(1) atom does not reveal such an effect.

Table 4. *Ratios of B_{eq} at two temperatures for $RbHSeO_4$ and NH_4HSeO_4*

The two columns for $RbHSeO_4$ correspond to the atoms *A(I)* and *A(II)* which are equivalent in the *B*2 phase.

	$RbHSeO_4$ B_{383}/B_{293} (383:293 = 1.31)	NH_4HSeO_4 B_{400}/B_{293} (400:293 = 1.37)
Rb(1) [N(1)]	1.36 (4)	1.61 (9)
Rb(2) [N(2)]	1.31 (4), 1.30 (4)	1.59 (6)
Se(1)	1.33 (4)	1.6 (1)
Se(2)	1.28 (4), 1.25 (4)	1.7 (1)
O(1)	1.35 (5), 1.33 (5)	1.7 (1)
O(2)	1.31 (5), 1.26 (5)	1.6 (1)
O(3)	1.32 (5), 1.31 (5)	1.7 (1)
O(4)	1.32 (5), 1.31 (5)	1.5 (1)
O(5)	1.32 (5), 1.32 (5)	1.5 (1)
O(6)	1.32 (5), 1.36 (5)	1.6 (1)
$H(1)_2$	1.3 (1)	2.4 (7)
$H(1)_1$	1.8 (2)	2.0 (4)
H(2)	1.19 (7), 1.17 (7)	1.6 (2)

Comparison of isotropic equivalent thermal parameters of the O atoms indicates that B_{eq} of the O(1) atom is even less than that for the O(3) and O(5) atoms involved in the β bonds with ordered H atoms (Table 2). Table 4 lists ratios of B_{eq} upon changes of temperature for $RbHSeO_4$ and NH_4HSeO_4 crystals. B_{eq} of all the atoms except the $H(1)_1$ atom decreases similarly in each crystal with decreasing temperature. B_{eq} of the H(1) atom changes drastically. As for non-H atoms in the structure of $RbHSeO_4$ the changes of B_{eq} are proportional to the absolute temperature change. Only the $H(1)_1$ atom exhibits anomalous behaviour of B_{eq}, which is evidence that this atom is disordered in the paraelectric phase and that it is ordered during the ferroelectric phase transition. Increasing the temperature from 293 to 400 K in the paraelectric phase of NH_4HSeO_4 results in a similar increase of B_{eq} of all non-H atoms, but this increase is larger than one would expect from the fact that B_{eq} is proportional to the absolute temperature (Willis & Pryor, 1975). Violation of proportionality of B_{eq} in this case can be interpreted as a manifestation of the temperature dependence of force constants when the temperature becomes close to the superionic phase transition temperature $T = 417$ K (Moskvitch, Sukhovsky & Rozanov, 1984). At 427 K NH_4HSeO_4 crystals start to show damage.

In order to reveal positional atomic disorder one can also use the analysis of vibration amplitudes along strong bonds, Se—O bonds in our case. Hirshfield (1976) suggested the so-called 'rigid-bond'

Table 5. *R.m.s. displacement* $(\langle u^2 \rangle)^{1/2}$ (Å) *of atoms in* $RbHSeO_4$ *and* NH_4HSeO_4

$u_{A,B} = (\langle u^2_{A,B} \rangle)^{1/2}$ = r.m.s. displacement of the A atom towards the B atom.

	$RbHSeO_4$				NH_4HSeO_4			
	293 K		383 K		293 K		400 K	
	$u_{Se,O}$	$u_{O,Se}$	$u_{Se,O}$	$u_{O,Se}$	$u_{Se,O}$	$u_{O,Se}$	$u_{Se,O}$	$u_{O,Se}$
Se(1)—O(1)	0.147 (2)	0.153 (3)	0.165 (3)	0.160 (3)	0.143 (6)	0.157 (7)	0.182 (9)	0.178 (9)
—O(11)	0.143 (2)	0.147 (3)						
—O(2)	0.128 (2)	0.132 (3)	0.156 (3)	0.158 (3)	0.129 (6)	0.138 (7)	0.167 (9)	0.195 (9)
—O(22)	0.138 (2)	0.139 (3)						
Se(2)—O(3)	0.158 (2)	0.157 (3)	0.184 (2)	0.190 (3)	0.172 (5)	0.159 (7)	0.216 (7)	0.214 (9)
—O(4)	0.139 (2)	0.143 (3)	0.154 (2)	0.162 (3)	0.139 (5)	0.142 (7)	0.175 (7)	0.174 (9)
—O(5)	0.144 (2)	0.147 (3)	0.158 (2)	0.161 (2)	0.136 (5)	0.148 (7)	0.185 (7)	0.192 (9)
—O(6)	0.146 (2)	0.149 (3)	0.167 (2)	0.167 (4)	0.149 (5)	0.151 (7)	0.190 (7)	0.185 (9)
Se(22)—O(33)	0.165 (2)	0.167 (3)						
—O(44)	0.134 (2)	0.138 (3)						
—O(55)	0.137 (2)	0.140 (3)						
—O(66)	0.154 (2)	0.156 (3)						

postulate in order to check whether the structure parameters are refined correctly. For two atoms linked by a strong covalent bond a relative vibrational motion has a very small component along the bond, *i.e.* these two atoms have nearly equal mean-square vibration amplitudes along the bond $\langle u^2_{A,B} \rangle \simeq \langle u^2_{B,A} \rangle$. The deviation from this equality for first-row atoms should be less than about 0.001 Å^2. The value for bonds of octahedrally coordinated transition metals is about 0.003 Å^2 (Chandrasekhar & Bürgi, 1984).

Table 5 shows $(\langle u^2 \rangle)^{1/2}$ values for the Se and O atoms along the Se—O bonds for $RbHSeO_4$ and NH_4HSeO_4. In all cases the differences between $(\langle u^2_{Se} \rangle)^{1/2}$ and $(\langle u^2_O \rangle)^{1/2}$ do not exceed two standard deviations. This is also true for the Se(1)—O(1) bond. The only exception is a difference for the bond Se(1)—O(2) for NH_4HSeO_4 at 400 K, which is probably connected with the insufficient accuracy of the high-temperature data for this crystal. Note that at T = 293 K the thermal parameters of the Se and O atoms in the paraelectric phase of NH_4HSeO_4 with H(1)-atom disorder are close to the thermal parameters of the Se and O atoms in the ferroelectric phase of $RbHSeO_4$ at the same temperature and ordered H(1)-atom arrangement. Analysis of $(\langle u^2 \rangle)^{1/2}$ values indicates that the ellipsoid of the O(1) atom is not extended along the Se—O bond any more than the ellipsoids of the O(3) and O(5) atoms. There is no significant disorder in the O(1)-atom arrangement.

The above considerations show that the preferred model is that with anharmonic thermal motion of the H(1) atom on the hydrogen α bond, when the averaged H(1)-atom site lies on the twofold axis and the probability of the atom location, as the atom undergoes thermal vibration, is higher in the regions of the two minima of the potential. The difference between the two models under consideration lies in the time the H(1) atom spends at various points in space during the course of its thermal motion. From this viewpoint positional and thermal parameters of the H(1) atom obtained in refinement of the two-site model can be regarded as an estimation of the H(1)-atom parameters when it is located at one of the two potential minima, assuming that

$$\langle u_1^2 \rangle \simeq \langle u_2^2 \rangle + (\delta/2)^2,$$

where $\langle u_1^2 \rangle$ is the mean-square amplitude obtained for the single-site model, $\langle u_2^2 \rangle$ is that for the two-site model, and δ is the separation between $H(1)_2$ and $H(1')_2$ sites in the two-site model.

There is always correlation between structural parameters in the refinement of any of the models considered. If the static spatial disordering model is used one should bear in mind the strong correlation between positional parameters, which define the separation δ between the $H(1)_2$ and $H(1')_2$ sites, and the thermal parameters of these atoms. When there is a strong correlation between the refined parameters, the appropriate section of the minimized function exhibits a plateau of practically the same values of the function instead of an abrupt minimum, *i.e.* the function is insensitive to variation of the refined parameters. In this case the estimated standard deviations no longer provide a means of assessing errors when attempting to find correlating parameters (Muradyan, Radaev & Simonov, 1989). Analysis of the dependence of the type $wR = f(\rho_i, \rho_k)$, where ρ_i and ρ_k are correlating parameters, is required in the vicinity of the minimum of the minimized function. It is solely the results obtained from the construction of appropriate confidence intervals that can be used as a criterion of the accuracy of the correlating parameters. Fig. 5 shows dependences $wR = f(\delta/2)$ obtained for $RbHSeO_4$ and NH_4HSeO_4 crystals. Curves 1, 2, 3 were plotted for a discrete fixed set of values of the $\delta/2$ parameter during full refinement of the other parameters of the two-site model. The appropriate B_{eq} values for the H(1) atom obtained for these $\delta/2$ values are also presented. For comparison, curves 4 were plotted from the results of a similar refinement of the ferroelectric phase of

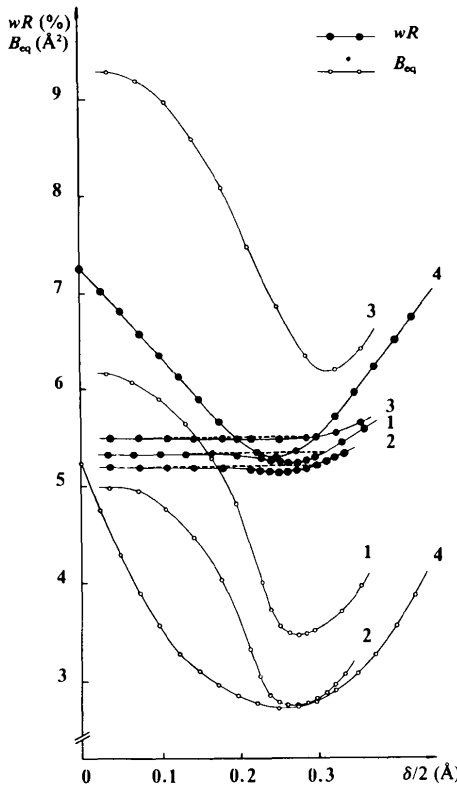

Fig. 5. The $\delta/2$ dependence of the weighted R factor (wR) and the equivalent isotropic thermal parameter (B_{eq}) for $RbHSeO_4$ at 383 K (curves 1), for NH_4HSeO_4 at 293 K (curves 2), for NH_4HSeO_4 at 400 K (curves 3), and for the ferroelectric phase of $RbHSeO_4$ at 293 K (curves 4).

$RbHSeO_4$. The wR dependence for the ferroelectric phase exhibits a sharp minimum corresponding to one H(1) site. The minima of the wR function of the two-site model refinement of the paraelectric phase are hardly expressed. In this case step-by-step scanning of the δ parameter provides a unique means of estimating the true value of δ. All the above dependences were plotted from neutron diffraction data with maximum $\sin\theta/\lambda = 0.79$ Å^{-1}. In this case the number of measured intensities of independent reflections N was different. For $RbHSeO_4$ at 383 K $N = 1069$, for NH_4HSeO_4 at 293 K $N = 744$, at 400 K $N = 532$. Obviously, a decrease in the number of independent reflections involved in the refinement is accompanied by an increase in the correlation between the refined parameters. In order to have more accurate structural information one should try to obtain the largest possible number of independent measurements for each parameter to be refined as well as increasing the limit of $\sin\theta/\lambda$.

The author would like to express her gratitude to Professor V. I. Simonov for helpful discussions, to Professor I. P. Aleksandrova for supplying the single crystals and for discussion of the results, and to Dr V. A. Sarin and Dr E. E. Rider for their assistance in carrying out the neutron measurements.

References

ALEKSANDROV, K. S., KRUGLIK, A. I., MISUL, S. V. & SIMONOV, M. A. (1980). *Kristallografiya*, **25**, 1142–1147.

ALEKSANDROVA, I. P., BLAT, D. KH., ZINENKO, V. I., MOSKVITCH, Y. N. & SUKHOVSKY, A. A. (1987). *Izv. Akad. Nauk SSSR Fiz.* **51**, 1688–1698.

BECKER, P. J. & COPPENS, P. (1974). *Acta Cryst.* A**30**, 129–147.

BRACH, I., JONES, D. J. & ROZIERE, J. (1983). *J. Solid State Chem.* **48**, 401–406.

CHANDRASEKHAR, K. & BÜRGI, H. B. (1984). *Acta Cryst.* B**40**, 387–397.

CZAPLA, Z. (1982). *Acta Phys. Pol. A*, **61**, 47–51.

CZAPLA, Z., LIS, T. & SOBCZYK, L. (1979). *Phys. Status Solidi A*, **51**, 609–612.

CZAPLA, Z., LIS, T., SOBCZYK, L., WAŚKOWSKA, A., MROZ, J. & PROPRAWSKI, R. (1980). *Ferroelectrics*, **26**, 771–774.

HIRSHFIELD, F. L. (1976). *Acta Cryst.* A**32**, 239–244.

KONDRATYUK, I. P., LOSHMANOV, A. A., MURADYAN, L. A., MAKSIMOV, B. A., SIROTA, M. I., KRIVANDINA, E. A. & SOBOLEV, B. P. (1988). *Kristallografiya*, **33**, 105–110.

KRUGLIK, A. I., MISUL, S. V. & ALEKSANDROV, K. S. (1980). *Dokl. Akad. Nauk SSSR*, **255**, 344–348.

MAKAROVA, I. P., MURADYAN, L. A., RIDER, E. E., SARIN, V. A., ALEKSANDROVA, I. P. & SIMONOV, V. I. (1990). *Kristallografiya*, **35**, 647–657.

MAKAROVA, I. P., RIDER, E. E., SARIN, V. A., ALEKSANDROVA, I. P. & SIMONOV, V. I. (1989). *Kristallografiya*, **34**, 853–861.

MOSKVITCH, Y. N., SUKHOVSKY, A. A. & ROZANOV. O. V. (1984). *Fiz. Tverd. Tela*, **26**, 38–44.

MURADYAN, L. A., RADAEV, S. F. & SIMONOV, V. I. (1989). *Methods of Structural Anlaysis*, edited by B. K. VAINSHTEIN, pp. 5–20. Moscow: Nauka.

MURADYAN, L. A., SIROTA, M. I., MAKAROVA, I. P. & SIMONOV, V. I. (1985). *Kristallografiya*, **30**, 258–266.

POPRAWSKI, R., MROZ, J., CZAPLA, Z. & SOBCZYK, L. (1979). *Acta Phys. Pol. A*, **55**, 641–646.

ROZANOV, O. V., MOSKVITCH, Y. N. & SUKHOVSKY, A. A. (1983). *Fiz. Tverd. Tela*, **25**, 376–380.

ROZANOV, O. V., MOSKVITCH, Y. N., SUKHOVSKY, A. A. & ALEKSANDROVA, I. P. (1983). *Izv. Akad. Nauk SSSR Fiz.* **47**, 719–722.

SIROTA, M. I. & MAKSIMOV, B. A. (1984). *Kristallografiya*, **29**, 34–38.

SUZUKI, S., OSAKA, T. & MAKITA, Y. (1979). *J. Phys. Soc. Jpn*, **47**, 1741–1742.

WAŚKOWSKA, A., OLEJNIK, S., ŁUKASZEWICZ, K. & CZAPLA, Z. (1980). *Cryst. Struct. Commun.* **9**, 663–669.

WAŚKOWSKA, A., OLEJNIK, S., ŁUKASZEWICZ, K. & GŁOWIAK, T. (1978). *Acta Cryst.* B**34**, 3344–3346.

WILLIS, B. T. M. & PRYOR, A. W. (1975). *Thermal Vibrations in Crystallography*, pp. 122–140. Cambridge Univ. Press.

ZUCKER, U. H., PERENTHALER, E., KUHS, W. F., BACHMANN, R. & SCHULZ, H. (1983). *J. Appl. Cryst.* **16**, 358.